Impact of Reactive Compatibilizers on the Properties of Poly(lactic acid)/Bamboo Flour Composites

Shuyu Zhao,[a,#] Qingqing Yang,[a,#] Lifen Li,[a,*] Yan Cao,[b,*] Yang Yang,[a] and Yaxue Wang [a]

The preparation of biodegradable wood plastic composites using polylactic acid (PLA) as the matrix and plant flours as the reinforcing phase aligns with the principles of sustainable development. However, there is a large polarity difference and poor compatibility between PLA and plant flours. To improve the performance of PLA/bamboo flour (BF) composites and simplify the process, this study modified PLA using glycidyl methacrylate (GMA), methacrylic acid (MAA), and maleic anhydride (MAH) as reactive compatibilizers. Composites were prepared from the modified PLA and BF using the hot-pressing method. The results indicated that all three reactive compatibilizers increased the polarity and surface free energy of PLA. GMA, MAA, and MAH were successfully grafted onto the PLA molecular chain, resulting in the formation of PLA-*g*-GMA, PLA-*g*-MAA, and PLA-*g*-MAH graft copolymers. In addition, the interfacial compatibility between PLA-*g*-GMA and BF was the best, and the PLA-*g*-GMA/BF composite had the lowest 24 h water absorption (2.17%). Furthermore, the PLA-*g*-GMA/BF composite showed the highest bending, tensile and impact strengths of 33.3 MPa, 14.7 MPa, and 1.33 kJ/m^2, respectively, which were 63.8%, 104.9% and 4.7% higher than those of untreated PLA/BF composites, respectively.

DOI: 10.15376/biores.20.3.5514-5532

Keywords: Polylactic acid; Wood plastic composites; Glycidyl methacrylate; Maleic anhydride; Methacrylic acid

Contact information: a: College of Forestry, Guizhou University, Guiyang 550025, Guizhou, China;
b: Special and Key Laboratory for Development and Utilization of Guizhou Superior Bio-based Materials, Guizhou Minzu University, Guiyang 550025, Guizhou, China;
** Corresponding author: lifenli2011@163.com; 02190707@163.com*

INTRODUCTION

Bamboo plants are known for their rapid growth, short life cycle, and excellent ecological performance. However, the current level of bamboo processing and utilization is still low, and it is estimated that the proportion of harvested bamboo material that is used in the production of bamboo building materials, bamboo furniture, and bamboo daily necessities is only 30% to 60% (Huang *et al.* 2023). At present, most of these residues are not reasonably utilized and are generally discarded or used as low-value fuel sources, resulting in serious resource waste and environmental pollution. Therefore, it is crucial to find high-quality and effective ways for utilizing bamboo processing residues in order to improve the comprehensive utilization rate of bamboo and mitigate the imbalance between wood supply and demand.

Wood plastic composites (WPCs) combine the properties of wood and plastic, offering excellent mechanical strength and environmentally benefits (Zhao *et al.* 2024).

These materials are widely applied in fields such as interior decoration, automotive interiors, aircraft components, biomedical, and garden landscaping (Avci *et al.* 2022). In recent years, WPCs have become a key research focus in the field of composites. However, the most common matrices used in WPC, such as polyethylene, polypropylene, and polyvinyl chloride, are derived from petroleum and are non-degradable. When discarded, these materials decompose into micro-plastics and nano-plastics under the effects of erosion and ultraviolet light, but cannot be digested by natural organisms. Meanwhile, due to the complexity of the matrix, WPCs are difficult to be reused through traditional plastic recycling methods (Chan *et al.* 2020).

A promising solution to this issue is the use of biodegradable plastics in WPC production. This approach not only reduces reliance on petroleum-based resources but also aligns with the objectives of a low-carbon economy. Common bio-based plastics, such as polylactic acid (PLA) (Parikh *et al*. 2024), polyhydroxyalkanoates (PHA) (Read *et al*. 2024), polybutylene succinate (PBS) (Rajgond *et al*. 2024), polyhydroxybutyrate (PHB) (Chen *et al*. 2025), and polybutylene adipate terephthalate (PBAT) (Shu *et al*. 2025) offer environmentally friendly alternatives. Among these, PLA, which is derived from lactic acid and produced using renewable resources like grains and crop residues, exhibits considerable potential. With favorable processing properties and good physical-mechanical properties, PLA shows great potential in areas such as packaging, disposable tableware, and automobile interiors, *etc*. It is considered one of the most promising renewable green polymers (Trivedi *et al*. 2023). However, PLA suffers from limitations such as high brittleness, poor impact resistance, high price and slow degradation rates (Liu *et al*. 2024), which limits its application in more fields.

Reinforcing PLA with plant fibers, such as straw, wood flour, and bamboo flour, can significantly reduce costs while improving its physical and mechanical performance (Hubbe *et al*. 2021; Wan *et al*. 2023). Composites prepared from PLA reinforced with bamboo fibers and other lignocellulosic materials exhibit good stability at room temperature, meet practical use requirements, and are fully degradable into CO_2 and H_2O under composting conditions (Rajeshkumar *et al.* 2021). This makes them environmentally benign after disposal, aligning with the principles of sustainable development. The interfacial adhesion between lignocellulosic fibers and plastic matrix plays a critical role in determining the macroscopic properties of WPCs (Song *et al.* 2017). However, the poor interfacial adhesion between the weaker polarity PLA and the stronger polarity plant fibers resulted in low interfacial strength and poor overall performance of the composites, which limiting the application of the composites. At present, in order to improve the interfacial compatibility between PLA and plant fibers, various methods such as fibers surface treatment, PLA modification, and the addition of specific additives can be applied (Prasad and Kumar 2016; Zhou *et al*. 2016; Omodunbi 2021). Conventional physicochemical modification methods, such as plasma treatment (Ma *et al.* 2025), alkali treatment (Avci *et al.* 2023), and maleic anhydride (Khamedi *et al.* 2019), can improve the interfacial compatibility between the two phases of the composites to a certain extent. However, these methods often present drawbacks including short residence time, environmental pollution, high energy consumption, and elevated processing costs (Ashraf et al. 2025; Elsheikh *et al.* 2022).

The development of environmentally friendly and efficient methods for interfacial modification of PLA/wood fiber is crucial for the fabrication of high-performance biodegradable WPCs. Recent studies have explored the use of graft copolymers such as PLA-*g*-GMA and PLA-*g*-MAH as reactive compatibilizers to improve the interfacial

compatibility and physico-mechanical properties of WPCs. Wu (2018) found that composites made with PLA-*g*-GMA and coupling agent-treated arrowroot fibers (AF) exhibited superior water resistance and mechanical properties compared to PLA/AF composites, where the tensile strength of PLA-*g*-GMA/TAF was 13-41 MPa higher than that of PLA/AF. Similarly, Zhang *et al.* (2017) used MAH as the graft monomer and employed a twin-screw extruder with di-tert-butyl peroxide (DCP) as an initiator to promote the grafting of MAH onto PLA. They successfully prepared WPCs by blending PLA, wood fibers, and PLA-*g*-MAH, resulting in enhanced tensile and bending strengths, with optimal properties achieved at a 30% PLA-*g*-MAH content. Compared to traditional interfacial modification methods, compatibilizer modification offers several advantages, including reduced use of chemical reagents, a simpler process, and greater cost-effectiveness. These benefits make it a promising option for practical industrial applications.

In this study, solid-phase grafting modification of PLA, using initiator benzoyl peroxide (BPO) as an initiator, was employed to prepare copolymers with glycerol methacrylate (GMA), methacrylic acid (MAA), and maleic anhydride (MAH), which represent epoxy, carboxylic acid, and anhydride-based reactive compatibilizers, respectively. The chemical composition of the copolymers was characterized using modern chemical analysis techniques, and the reaction pathways between the compatibilizers and PLA were deduced. The interfacial compatibility and the physical-mechanical properties of the copolymers/BF composites, which were prepared using the hot-pressing method, were investigated. This research provides theoretical insights and experimental evidence for the development of fully biodegradable PLA/lignocellulosic fiber composites with enhanced comprehensive performance.

EXPERIMENTAL

Reagents and Materials

Bamboo processing residues were purchased from Longmen County, Huizhou City, Guangdong Province, China. Polylactic acid powder (PLA), model 4032D, was purchased from Nature Works Company, USA. Benzoyl peroxide (BPO), polyethylene grafted maleic anhydride (MAH), glycidyl methacrylate (GMA), and methacrylic acid (MAA) were purchased from Aladdin Biochemical Technology Co., Ltd., Shanghai, China.

Preparation of Bamboo Plastic Composites

Reactive compatibilizer modification treatment of PLA

The reactive compatibilizer modification of PLA was carried out using glycidyl methacrylate (GMA), methacrylic acid (MAA), and maleic anhydride (MAH). Each compatibilizer was separately mixed with the initiator benzoyl peroxide (BPO) at a mass ratio of 10: 1 in a high-speed mixer (SHR-5, Suzhou Chaoweier Machinery Co., Ltd., Suzhou, China). PLA was heated in a stirrer at 80 °C and 30 rpm for 5 min. Following a compatibilizer concentration of 3% (by mass) relative to bamboo plastic composites (BPCs), the compatibilizer/BPO mixture was gradually added to the PLA and compounded for an additional 3 min to form PLA graft copolymers. The graft copolymers obtained with the three different reactive compatibilizers were defined as PLA-*g*-GMA, PLA-*g*-MAA and PLA-*g*-MAH, respectively.

Preparation of PLA/bamboo flour composites

Pre-dried bamboo flour (BF) was mixed with untreated and modified PLA in a high-speed mixer (SHR-5, Suzhou Chaoweier Machinery Co., Ltd., Suzhou, China) at a mass ratio of 2: 8. The mixture was stirred at 100 ℃ and 50 rpm for 5 min. The blended mixture was then placed in a 22 × 22 × 4 cm mold and subjected to hot pressing in a plate vulcanizer (XLB-100, Yangzhou Zhengyi Testing Machinery Co. Ltd., Yangzhou, China). Preheating was carried out at 180 ℃ with a pressure range of 1 to 2 MPa for 8 min, after which the pressure was increased to 4 to 5 MPa for an additional 15 min. After the pressure was released, the composites were allowed to cool overnight. The design density of the composite was 1.2 g/cm^3. The BPCs prepared with PLA-*g*-GMA, PLA-*g*-MAA, and PLA-*g*-MAH, in combination with BF, were referred to as PLA-*g*-GMA/BF, PLA-*g*-MAA/BF, and PLA-*g*-MAH/BF, respectively.

Surface Polarity and Chemical Structure Analysis of Polylactic Acid

Surface polarity testing

The surface polarity of BF, as well as untreated and modified PLA, was analyzed using the tablet method. Before the test, a small amount of BF, modified PLA, and untreated PLA was taken and pressed into uniformly thick sheets using a flour tablet press at a pressure of 20 to 40 MPa for 5 min. The contact angle of BF and PLA was measured using a contact angle meter (JC2000A, Chengde Jinhe Instrument Manufacturing Co., Ltd., China) with distilled water and ethylene glycol as the test liquids. The surface polarity component, dispersion component and surface free energy of both BF and PLA, before and after modification, were calculated according to Eqs. 1 and 2.

$$r_1(1 + cos\theta) = 2[(r_f^p r_l^p)^{\frac{1}{2}} + (r_f^d r_l^d)^{\frac{1}{2}}] \quad (1)$$

$$r_f = r_f^p + r_f^d \quad (2)$$

where r_1 denotes the surface energy of the testing liquid, θ denotes the contact angle (°) between the testing liquid and the flour, r_{pl} denotes the polar component of the surface energy of the testing liquid, r_{dl} denotes the dispersion component of the surface energy of the testing liquid, r_{pf} denotes the polar component of the surface energy of the flour, r_{df} denotes the dispersion component of the surface energy of the flour, r_f denotes the surface free energy of the flour.

Chemical structure analysis of polylactic acid

The chemical structure of PLA was analyzed using Fourier transform infrared (FTIR) spectroscopy and hydrogen nuclear magnetic resonance (^{1}H NMR) spectroscopy. FTIR analysis was conducted on both untreated and modified PLA using the potassium bromide (KBr) compression method. The PLA samples were milled and mixed with KBr at a mass ratio of 1: 100 and then pressed into translucent pellets. These pellets were tested using a FTIR spectrometer (Nicolet 6700, Thermo Fisher Scientific, USA) within the range of 4000 to 400 cm^{-1}, with 32 scans and a spectral resolution of 4 cm^{-1}. For ^{1}H NMR analysis, both modified and untreated PLA samples were dissolved in deuterated chloroform and analyzed using a 600 MHz NMR spectrometer (Q.One Instruments Ltd., Wuhan, China) with tetramethylsilane (TMS) as an internal standard.

A brief flowchart of the PLA modification and testing is shown in Fig. 1.

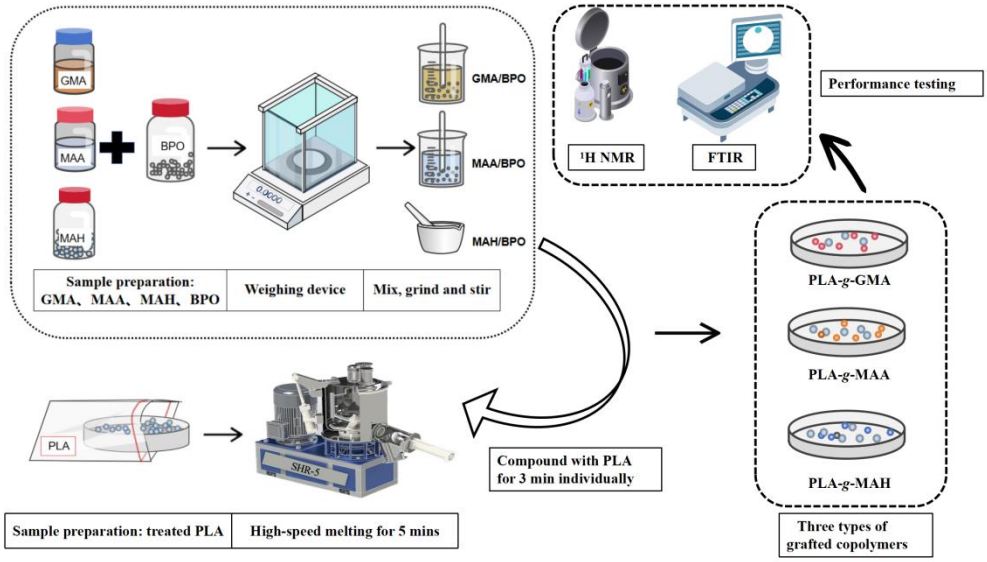

Fig. 1. Flow chart of PLA modification and testing

Micro-morphological Analysis of Composites

Scanning electron microscope (SEM) was employed to observe the micro-morphology of the impact sections of the specimens and to analyze the microstructure and micropore characteristics of the different composite groups. For the SEM tests, the composites samples were cut into 10 mm × 10 mm × 1 mm specimens, which were then mounted on conductive adhesive and gold-coated for 45 s using an Oxford Quorum SC7620 sputter coater at a current of 10 mA. After gold spraying, these specimens were examined in a SEM (GeminiSEM 300, Carl Zeiss AG, Oberkochen, Germany) at an accelerating voltage of 12.5 kV, and the images were saved for further analysis.

Water Absorption and Mechanical Properties Test for Composites

Water absorption test for composites

The water absorption of PLA/BF composites was tested according to GB/T 17657 (2022). Specimens measuring 50 mm × 50 mm × 4 mm were immersed in a water bath at 20 °C. After the predetermined time, the specimens were removed, and excess surface water was carefully wiped off with a soft cloth before weighing. The results of each set of specimens were averaged over four replicates.

Mechanical properties test for composites

The flexural properties of the composites was tested According to GB/T 17657 (2022). A three-point bending test was performed using a universal material tensile testing machine (LGS20K, Xiamen Yishite Instruments Co. Ltd., Xiamen, China) to evaluate the bending strength and bending modulus. The specimen size was 80 mm × 13 mm × 4 mm, with a span of 64 mm. The loading speed of the bending force was set to 2.0 mm/min and the average value of five samples in each group was taken as the final result.

The tensile properties of the composites were tested according to GB/T1040.1-(2006). Dumbbell-type (I type) specimens measuring 150 mm × 20 mm × 4 mm were prepared using a dumbbell-type sample making machine (FBS-25Y, Shenzhen Fobus Instrument Co., Ltd., Shenzhen, China). During the test, the samples were clamped in a universal tensile testing machine (LGS20K, Xiamen Yishite Instruments Co. Ltd., Xiamen, China), with a tensile force speed set to 5 mm/min to measure the tensile strength and

tensile modulus. Each group was tested five times, and the average value was taken as the final result.

The impact properties of the composites were evaluated according to GB/T 1043.1 (2008). Simply supported beam pendulum impact tests were performed on the specimens using an impact tester (XJUD-22, Chengde Wansu Testing Instrument Co., Ltd., Chengde, China). The test span was set to 60 mm, with an impact velocity of 2.9 m/s and a pendulum energy of 2 J. The specimen size was 80 mm × 10 mm × 4 mm, with no notch. For each impact properties test, the average value of five samples was taken as the result.

A brief flowchart of the BPCs production process and testing is shown in Fig. 2.

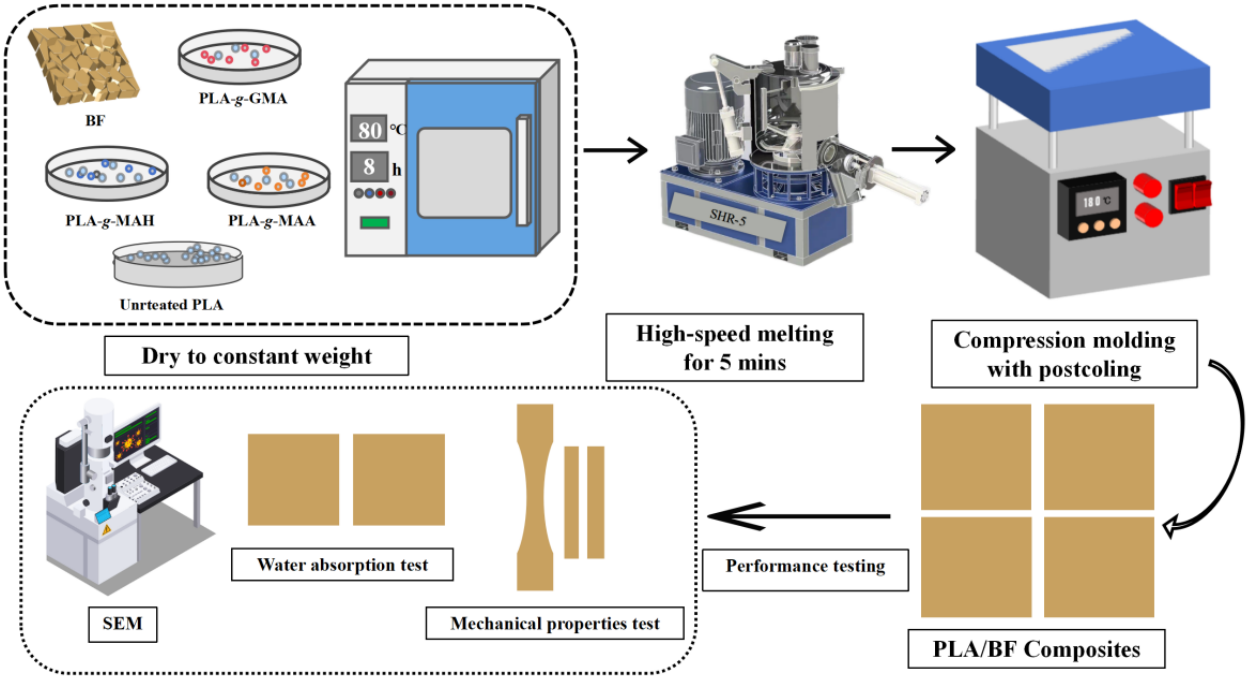

Fig. 2. Production and testing flowchart of BPCs

Statistical Analysis

One-way analysis of variance (ANOVA) and least significant difference (LSD) multiple comparison tests were performed using SPSS version 26.0 to assess significant differences ($p < 0.05$) between the results.

RESULTS AND DISCUSSION

Effect of Compatibilizers Modification on the Surface Polarity and Surface Free Energy of PLA

The variations in surface free energy and surface polarity between lignocellulosic fiber materials and plastic matrices significantly play a crucial role in determining the interface of WPCs, as well as their physical and mechanical properties (Gupta *et al*. 2007; Meng *et al*. 2024). The surface polarity and surface free energy of PLA, PLA-*g*-GMA, PLA-*g*-MAA, PLA-*g*-MAH, and BF were analyzed and calculated using distilled water and ethylene glycol as probe liquids, and the results are shown in Table 1. The surface polarity and surface free energy of PLA were 8.3 and 25.7 $mJ \cdot m^{-2}$, respectively, while those of BF were 38.4 and 47.5 $mJ \cdot m^{-2}$, respectively, indicating a significant difference in polarity between the two materials. The surface polarity component and surface free energy of PLA increased after modification with GMA, MAA, and MAH. Among the various copolymers studied, PLA-*g*-MAH had the highest surface polarity component and surface free energy of 22.7 and 42.1 $mJ \cdot m^{-2}$, respectively. The surface polarity component and surface free energy of PLA-*g*-GMA were 13.8 and 27.8 $mJ \cdot m^{-2}$, respectively, showing an increase compared to PLA. In contrast, the surface polarity component and surface free energy of PLA-*g*-MAA were relatively lower, at 12.8 and 26.6 $mJ \cdot m^{-2}$, respectively.

Table 1. Contact Angle and Surface Free Energy of PLA

Sample Types	Contact angle of distilled water (°)	Glycol contact angle (°)	Dispersion component ($mJ \cdot m^{-2}$)	Polar component ($mJ \cdot m^{-2}$)	Surface free energy ($mJ \cdot m^{-2}$)
Untreated PLA	84.2	63.0	17.4	8.3	25.7
PLA-*g*-GMA	78.0	59.5	13.9	13.8	27.8
PLA-*g*-MAA	79.8	61.5	13.74	12.8	26.6
PLA-*g*-MAH	60.5	32.0	19.4	22.7	42.1
BF	53.0	37.0	9.0	38.4	47.5

Effect of Compatibilizers Modification on the Chemical Structure of PLA

FTIR spectroscopy and ^{1}H NMR were used to analyze the changes in the chemical structure of PLA before and after modification with a compatibilizer. The results are shown in Figs. 3 and 4.

Figure 3 shows the FTIR spectra of both untreated PLA and modified PLA. It can be observed that both modified and untreated PLA exhibited an O-H stretching vibration peak at 3461 cm^{-1}, a C-H stretching vibration absorbance peak at 2817 cm^{-1}, a strong absorbance band at 1750 cm^{-1} corresponding to the stretching vibration absorbance peak of the carboxyl group (C=O) in the PLA main chain, and C-H in-plane bending vibration absorbance peaks at 1461 and 1368 cm^{-1}. GMA, a reactive epoxy compatibilizer, showed a characteristic infrared absorbance peak of the epoxy group around 910 cm^{-1} (Sajna *et al.* 2016). This group is an important indicator to determine whether PLA and GMA have successfully grafted (Guo *et al*. 2020).

The blend of PLA and GMA after reaction showed a distinct epoxy characteristic peak at this position. Besides, the absence of characteristic signal peaks for C=C in GMA (3140, 1640, 940, and 815 cm^{-1}) suggests that the GMA monomer is not retained in the test material (Martel *et al*. 2000). Therefore, the epoxy absorbance peak observed here originated from the successfully grafted PLA-*g*-GMA. On the other hand, MAH, an

anhydride-type compatibilizer, showed two distinct anhydride characteristic absorbance peaks at 1785 and 1806 cm^{-1} in the modified PLA, corresponding to the asymmetric and symmetric stretching vibration peaks of the C=O in MAH, respectively. No such peaks were observed in pure PLA, indicating that MAH has been successfully grafted onto PLA (Jiang *et al*. 2013). Compared with the infrared spectrum of pure PLA, the infrared spectrum of the graft copolymer PLA-*g*-MAA showed a new absorbance peak located at 1680 cm^{-1}, which corresponds to the characteristic peak of carboxylic acid (C=O) and is attributed to the stretching vibration of the carbonyl C=O in MAA, indicating that MAA had been successfully grafted onto PLA.

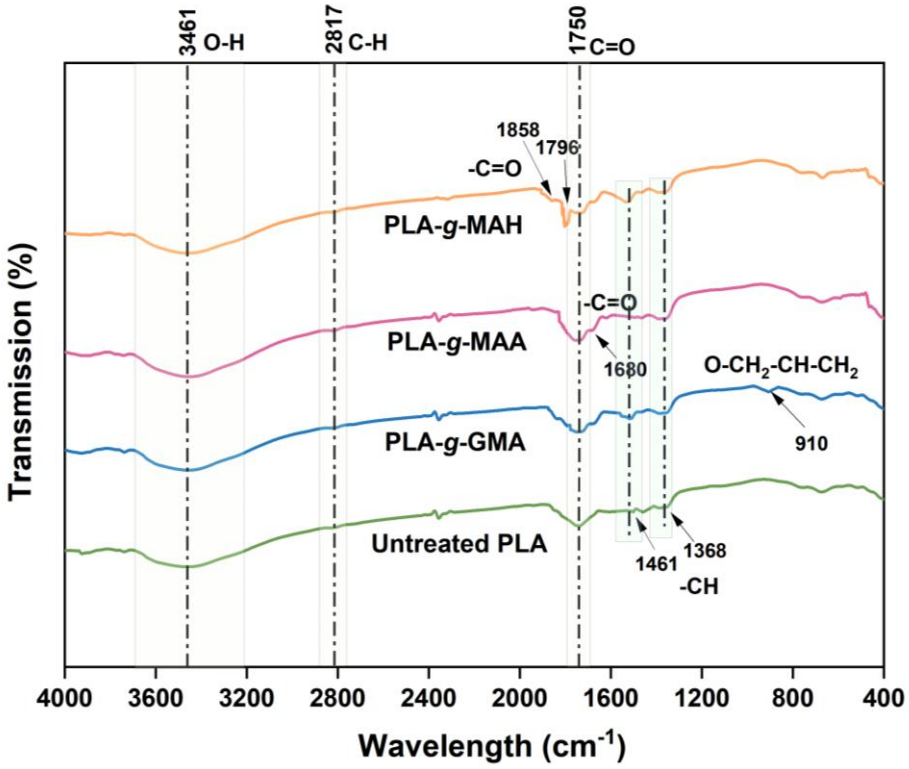

Fig. 3. Infrared spectra of unmodified and modified polylactic acid (PLA)

The results of ^{1}H NMR spectroscopy for untreated and modified PLA dissolved in deuterated chloroform (δ=7.260) are shown in Fig. 4. The characteristic signals of the methyl (-CH_3) and methylene (-CH-) protons in the PLA molecule appeared at δ=1.57 and 5.17 ppm, respectively (Pérez *et al*. 2022). The absorbance peaks at δ=0.25 and 1.25 corresponded to the methyl groups on GMA, confirming the successful preparation of PLA-*g*-GMA (Sajna *et al*. 2016). Small peaks between 6.13 and 6.47 ppm were attributed to the proton absorption of the unsaturated CH in MAH (Luo *et al*. 2022), indicating successful grafting of MAH onto PLA, although the small peak area suggests a low grafting rate. The series of small peaks observed between δ=0.86 and 1.24 were the methyl proton signals of MAA, while the methylene proton signal at δ=1.94 ppm was indicative of MAA, confirming its successful grafting onto PLA (Rodic *et al*. 2014). Liu *et al*. (2016) also found that proton signals in the 1.1 to 2 ppm range correspond to the -CH_2-CH_2-CH_2- group. These results indicate that GMA, MAH, and MAA monomers underwent graft copolymerization with PLA during the blending process. On the other hand, the characteristic proton signal peaks near 5.6 and 6.1 ppm, corresponding to CH_2=C- in the

GMA monomer (Lainé *et al*. 2008), the main chain C-H proton signal near 3.73 ppm for the MAH monomer (Atabaki *et al*. 2018), and the allyl proton signals near 5.4 and 5.9 ppm for the MAA monomer (Liu *et al*. 2016), were not observed. This absence indicates that GMA, MAH, and MAA monomers were not present in the copolymer.

Combined with FTIR and ^{1}H NMR analysis, these results confirmed that GMA, MAA and MAH were successfully grafted onto PLA under the action of BPO initiator, and that there were no free monomers in the grafted polymer.

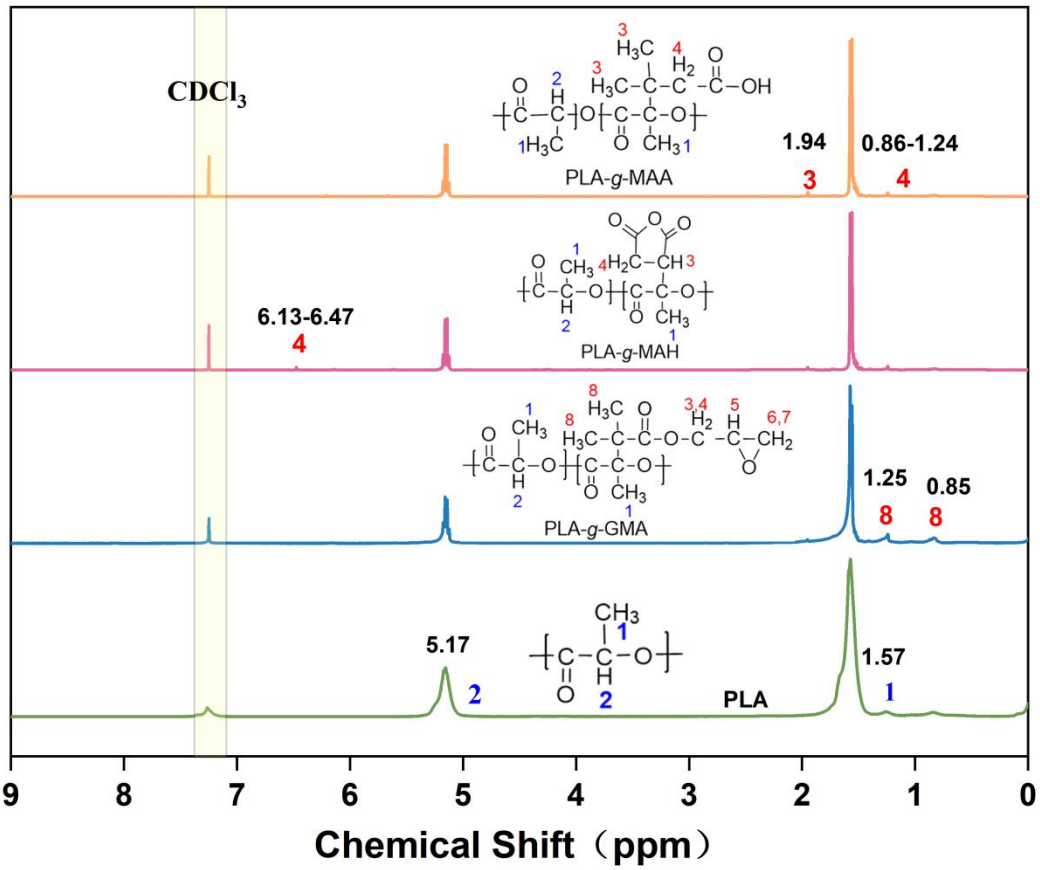

Fig. 4. ^{1}H NMR spectra of unmodified and modified polylactic acid (PLA)

The possible reaction pathways of GMA, MAA, and MAH with PLA were hypothesized in the light of the relevant literature (Xu *et al*. 2012; Han *et al*. 2021) as well as the results of FTIR spectroscopy and ^{1}H NMR analysis. It is proposed that, initially, the initiator BPO decomposed at high temperatures to generate peroxide radicals (Fig. 5a). These peroxide radicals extracted hydrogen atoms from the tertiary carbon atoms in PLA molecules, leading to the formation of stable macromolecular radicals (Fig. 5b). Subsequently, the PLA macromolecular radicals attacked the C=C bonds in GMA, MAA, and MAH, resulting in the grafting of these monomers onto the PLA molecular backbone, forming PLA-*g*-GMA, PLA-*g*-MAA, and PLA-*g*-MAH (Fig. 5c).

Effect of Compatibilizer Modification on the Microscopic Morphology of PLA/BF Composites

The microscopic morphology of composites is an important method for evaluating

their interfacial compatibility. The SEM images of the impact fracture surface of PLA/BF composites are shown in Fig. 6. As shown in Fig. 6a, BF was distributed in a strip-like shape within the pure PLA matrix, exhibiting relatively large dimensions and an intact structure. The fracture surface exhibited numerous deep holes and noticeable defects, indicating poor interfacial adhesion between BF and untreated PLA. Under external forces, the BF was observed to slip out of the PLA matrix, failing to contribute to the reinforcement of the composite and unable to share the stress of the PLA matrix.

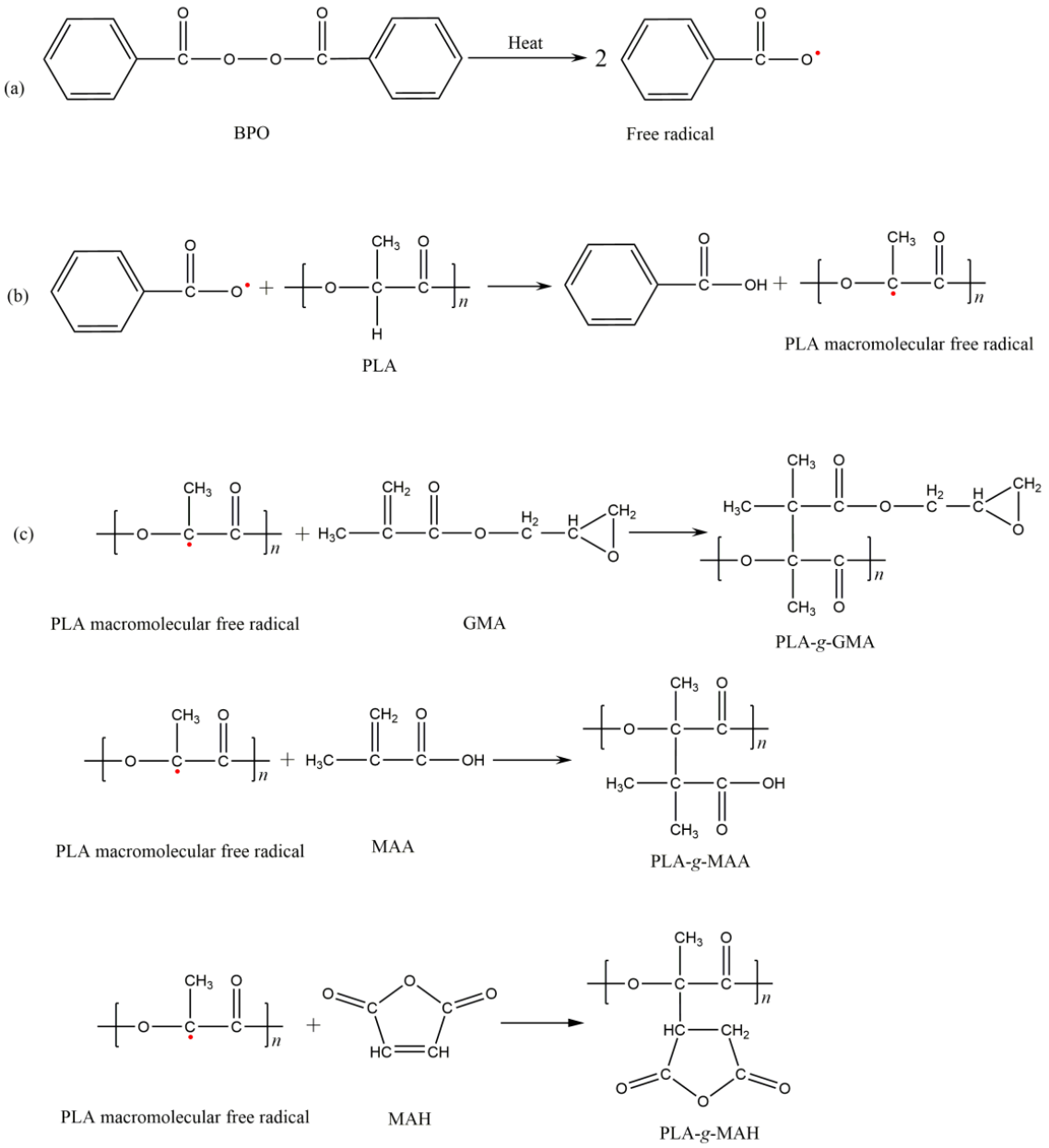

Fig. 5. Possible reaction pathways of PLA with GMA, MAH, and MAA

However, in the case of the PLA-g-GMA/BF composite (Fig. 6b), which underwent the same hot-pressing process, the fracture surface displayed a reduction in the number of pores, improved structural integrity, and visible tearing of some BF at the fracture site. This

indicates that stress was effectively transferred from the PLA matrix to the BF, enabling the flours to take on a load-bearing role under external force, which led to their fracture and damage. In addition, the dispersion of BF in PLA-*g*-GMA/BF was notably improved, and the interfacial phase between BF and PLA-*g*-GMA was not obvious, indicating enhanced interfacial bonding and superior compatibility. For composites prepared with MAH- and MAA-modified PLA (Fig. 6c and 6d), some of the BF exhibited aggregation, and the number of voids was higher, suggesting that the interfacial compatibility of PLA-*g*-MAH and PLA-*g*-MAA was not as effective as in the PLA-*g*-GMA/BF composites.

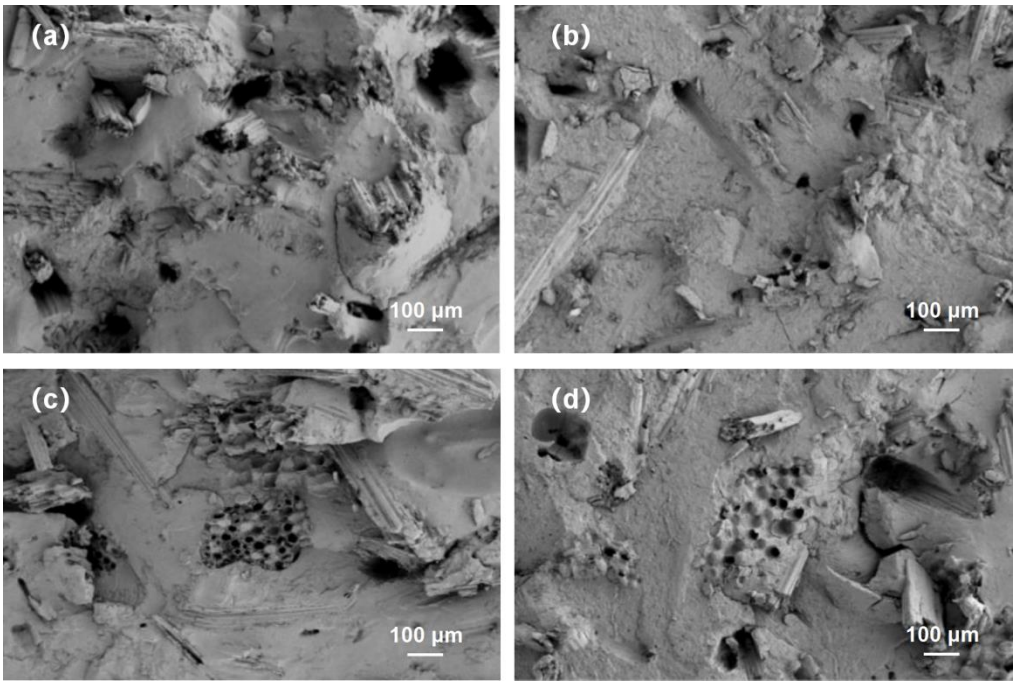

Fig. 6. Scanning electron micrographs of BPCs: (a) PLA/bamboo composite; (b) PLA-g-GMA/bamboo composite; (c) PLA-g-MAA/bamboo composite; (d) PLA-g-MAH/bamboo composite

Effect of Compatibilizer Modification on Water Absorption of PLA/BF Composites

The results of 24 h water absorption tests and the changes in water absorption rates over time of the composites prepared using PLA modified with different reactive compatibilizers are shown in Fig. 7. As the soaking time of the composites in water increased, the water absorption rates of all composites gradually increased. This was attributed mainly to the strong water-absorbing ability of BF. In addition, treatment of PLA with three compatibilizers reduced the water absorption of the composites to some extent. Among these, the PLA-*g*-GMA/BF composite showed the lowest 24 h water absorption (2.2%), which was 21.7% lower than that of the untreated composite (2.8%). The PLA-*g*-MAH/BF and PLA-*g*-MAA/BF composites showed water absorption percentages of 2.31% and 2.54%, respectively. The reduction in water absorption rate of the composites prepared with compatibilizer-modified PLA may be due to several reasons. The compatibilizer modification improves the compatibility between PLA and BF, which reduces the number of pore structures within the composites, thereby hindering the penetration of water molecules and lowering the overall water absorption. Microstructural analysis indicated that PLA-*g*-GMA/BF had the best interfacial compatibility, which likely contributed to its

lowest water absorption rate among the four BPCs. Additionally, the surface functional groups of the compatibilizers could chemically react with the hydroxyl groups on the surface of BF during the hot-pressing process, reducing the content of strongly polar hydroxyl groups on the BF surface and further reducing the hydrophilicity of the composite.

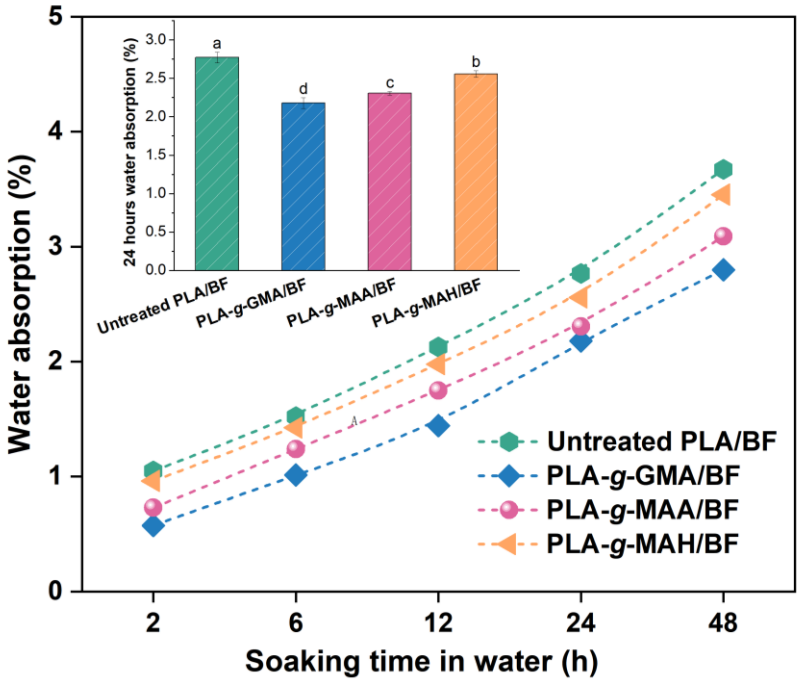

Fig. 7. Water absorption of compatibilizer modified BPCs. Values with the same letter are not significantly different (p<0.05).

Effect of Compatibilizer Modification on Mechanical Properties of PLA/BF Composites

Figure 8 shows the bending strength, modulus of elasticity, and stress-strain curves of PLA/BF composites. The GMA and MAA modification treatments improved the static bending strength and elastic modulus of the composites to a certain extent, with the GMA treatment showing the most significant improvement in the flexural properties. The bending strength of PLA-*g*-GMA/BF (33.3 MPa) increased by 63.8% compared to the untreated composites (20.4 MPa), and the modulus of elasticity (7.95 GPa) increased by 13.7% compared to the untreated group (6.99 GPa). The enhanced performance of the PLA-*g*-GMA/BF composites may be attributed to several factors. Microscopic analysis showed that the interfacial compatibility of PLA-*g*-GMA/BF was superior, which was likely due to the epoxy groups in PLA-*g*-GMA reacting with the hydroxyl groups on BF to form hydrogen bonds. The hydrogen bond enhances the interfacial bonding strength and stability, enabling more effective stress transfer from the PLA matrix to the BF under external forces, thereby reducing the internal stress concentration and improving the bending properties of the composite. Additionally, the polymerization of GMA with PLA can disrupt the regularity of the intermolecular arrangement of PLA. This would increase the spacing between PLA molecules, which enhances the toughness and plasticity of PLA, promoting better interpenetration and entanglement between PLA and BF, thereby forming a denser material structure. In contrast, the flexural properties of PLA-*g*-MAH/BF were

lower, which may be due to the relatively high addition of MAH used in this study. An excessive amount of PLA-*g*-MAH can remain in the PLA and BF, making the molecular chains more prone to sliding, which could lead to a reduction in the bending strength of the composites (Zhang *et al*. 2017).

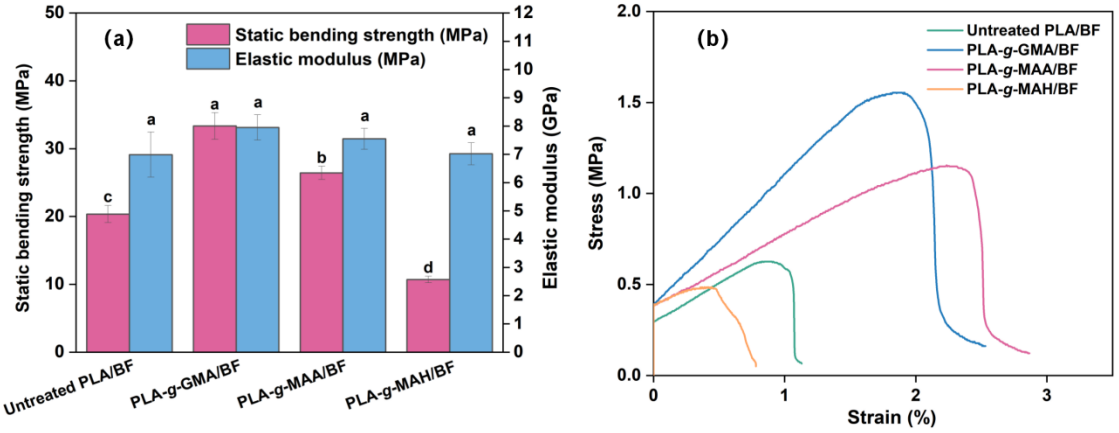

Fig. 8. Bending strength, modulus of elasticity (a) and stress-strain curves (b) of compatibilizer modified BPCs. Values with the same letter are not significantly different (p<0.05).

The tensile properties of BPCs can be significantly influenced by the modification of PLA with GMA, MAA, and MAH, as shown in Fig. 9. The PLA-*g*-GMA/BF composite showed the highest tensile strength at 14.7 MPa, representing an significant increase of 104.9% compared to the untreated group, which had a tensile strength of 7.17 MPa. However, this composite also showed the lowest elongation at break of 3.77%, a decrease of 10.0% from the untreated group's 4.19%. This reduction can be attributed to the highly reactive epoxy groups in GMA, which react with the hydroxyl groups on BF to form strong chemical bonds. These bonds enhance the intermolecular forces and create a cross-linked network structure that prevents stress concentration but restricts molecular motion. This leads to an increase in tensile strength while reducing elongation at break. Conversely, the PLA-*g*-MAH/BF composite showed the lowest tensile strength (4.56 MPa) and the highest elongation at break (4.67%), representing a 36.4% decrease of tensile strength and an 11.5% increase in elongation at break compared to the untreated group. This trend aligns with the changes observed in the static bending strength of the composites.

The higher elongation at break of PLA-*g*-MAH/BF may be because, although the molecular chains of PLA-*g*-MAH/BF tend to slide under external forces, which prevents the effective transfer of tensile stress from the PLA matrix to the BF and leads to a reduction in the tensile strength, this sliding enhances the ductility of the material, allowing it to withstand greater deformations without fracture.

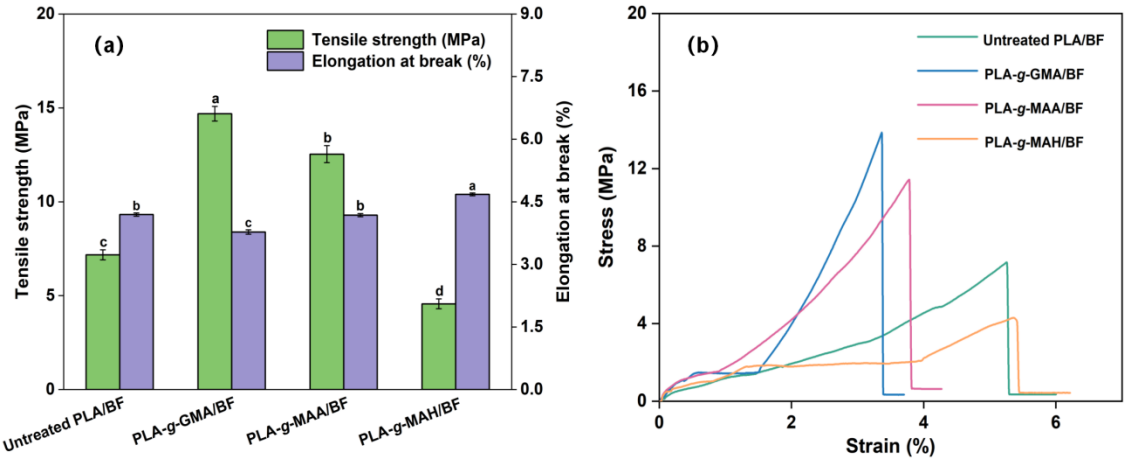

Fig. 9. Tensile strength, elongation at break (a) and stress-strain curves (b) of compatibilizer modified BPCs. Values with the same letter are not significantly different (p<0.05).

Figure 10 shows the impact strength of the PLA/BF composites. The PLA-*g*-GMA/BF composite had the best impact performance of 1.33 kJ/m^2, followed by the untreated PLA/BF and PLA-*g*-MAA/BF, while PLA-*g*-MAH/BF composite had the worst impact performance of 0.63 kJ/m^2. This is because GMA has the most effective impact on improving the compatibility between the two phases of the BF/PLA composite. After GMA compatibilization, the two phases are more efficiently bonded, which can absorb and disperse external force more effectively and reduce stress concentration, thus improving the impact performance. However, overall, the modification treatments with the three types of compatibilizers in this study did not significantly improve the impact performance of the BPCs.

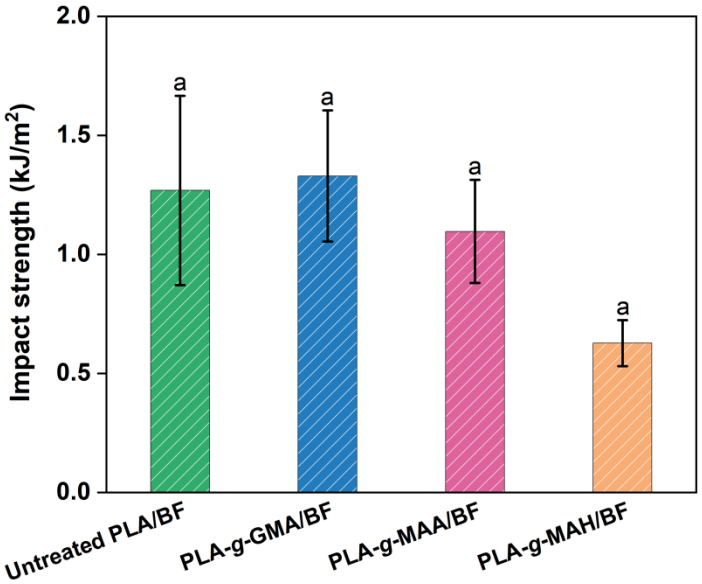

Fig. 10. Impact strength of compatibilizer modified BPCs. Values in each column followed by the same letter were not significant differences (p<0.05).

Mechanism of Compatibilization of GMA Modification on PLA/bamboo Flour Composites

In this study, PLA-*g*-GMA/BF had the best physical and mechanical properties, such as water absorption, bending, tensile and impact properties, among the several composites studied. This can be attributed to the high reactivity of the epoxy groups in GMA.

During the hot-pressing process, PLA-*g*-GMA can react with the hydroxyl groups in BF, reducing the hydroxyl content of BF while simultaneously enhancing the connection between PLA-*g*-GMA and BF. This enhances the interfacial compatibility between the two phases in the composites. The reaction mechanism is shown in Fig. 11.

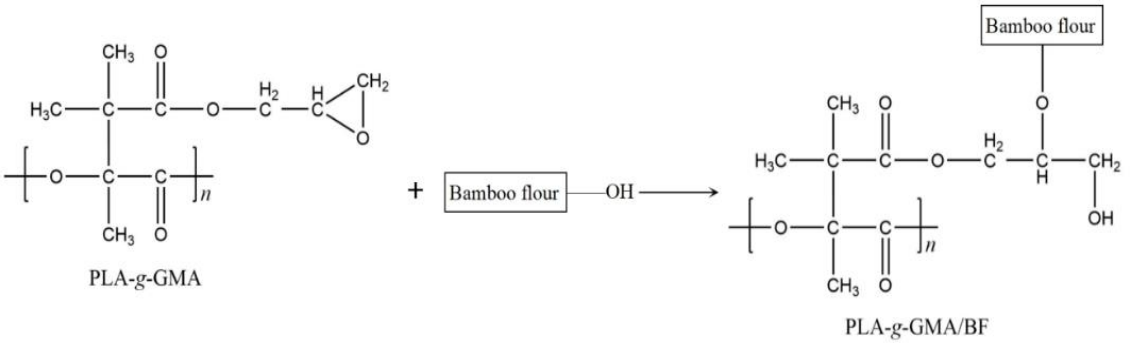

Fig. 11. Mechanism of bonding the PLA-g-GMA with hydroxyl group of BF

CONCLUSIONS

1. Glycidyl methacrylate (GMA), methacrylic acid (MAA), and maleic anhydride (MAH) were successfully grafted onto the poly(lactic acid) (PLA) molecular chain to form PLA-*g*-GMA, PLA-*g*-MAA, and PLA-*g*-MAH graft copolymers. The surface free energies of these copolymers were increased to different degrees compared to pure PLA. Among these, PLA-*g*-MAH had the highest surface free energy and polar component of 42.1 and 25.7 $mJ \cdot m^{-2}$, respectively.
2. The microscopic morphology of the composites with bamboo flour (BF) showed that untreated PLA/BF composites had larger and more intact reinforcement particles on the impact fracture surface, along with deeper holes in the matrix. Compatibilization modification improved the interfacial compatibility between PLA and BF to a certain extent, in which PLA-*g*-GMA/BF had the smoothest impact fracture surfaces with fewer voids and gaps, indicating better interfacial compatibility of this composites.
3. Compared with untreated PLA/BF composites, the GMA, MAA, and MAH-treated PLA all reduced the water absorption percentage of the BPCs. Among these, PLA-*g*-GMA/BF showed the lowest 24 h water absorption of 2.17%, which was 21.7% lower than that of the untreated composites (2.77%).
4. Compared to the untreated PLA/BF composites, GMA-, MAA-, and MAH-treated PLA altered the mechanical properties of the composites to varying degrees. Among these, PLA-*g*-GMA/BF showed the highest bending, tensile and impact strength of 33.3 MPa, 14.7 MPa, and 1.33 kJ/m^2, respectively, which represented increases by 63.8%, 104.9% and 4.7%, respectively, when compared with untreated PLA/BF composites. The MAA treatment moderately improved the mechanical properties of

BPCs, but the effects were less pronounced. In addition, PLA-*g*-MAH/BF showed the highest elongation at break of 4.67%, which was 11.5% greater than that of the untreated composites. However, the MAH treatment decreased the bending, tensile, and impact strength of the composites.

5. Among the three reactive compatibilizers, GMA graft-modified PLA showed the most significant enhancement in the physical and mechanical properties of BPCs. Therefore, GMA can be considered the preferred reactive compatibilizer for modifying PLA, offering promising prospects for the development of high-performance WPCs in future practical applications.

ACKNOWLEDGMENTS

The authors gratefully acknowledge the support of the Natural Science Foundation of Guizhou Province (No. Qiankehe ZK [2022] General 067), National Natural Science Foundation of China (32160413), International Joint Research Center for Biomass Materials, (Southwest Forestry University) (2023-GH06), the 111 Project (D21027), and the Student Research Training Program of Guizhou University (2024-312).

REFERENCES CITED

Ashraf, J., Bertin, M., and Verbeek, C. J. R. (2025). "Plasma-induced reactive compatibilization of polypropylene/polyamide 6 blends," *ACS Applied Polymer Materials* 7(2), 641-653. DOI: 10.1021/acsapm.4c02896

Atabaki, F., Shokrolahi, A., and Pahnavar, Z. (2018). "Methyl methacrylate based copolymers and terpolymers: Preparation, identification, and plasticizing capability for a poly(methyl methacrylate) used in aviation," *Journal of Applied Polymer Science* 135(34), article 46603. DOI: 10.1002/app.46603

Avci, A., Eker, A. A., Bodur, M. S., and Candan, Z. (2022). "An experimental investigation on the thermal and mechanical characterization of boron/flax/PLA sustainable composite," *Proceedings of the Institution of Mechanical Engineers Part L-Journal of Materia* 236(12), 2561-2573. DOI: 10.1177/14644207221121984

Avci, A., Eker, A. A., Bodur, M. S., and Candan, Z. (2023). "Water absorption characterization of boron compounds-reinforced PLA/flax fiber sustainable composite," *International Journal of Biological Macromolecules* 233, article 123546. DOI: 10.1016/j.ijbiomac.2023.123546

Chan, C. M., Vandi, L. J., Pratt, S., Halley, P., Richardson, D., Werker, A., and Laycock, B. (2020). "Mechanical stability of polyhydroxyalkanoate (PHA) based wood plastic composites (WPCs)" *Journal of Polymers and the Environment* 28(5), 1571-1577. DOI: 10.1007/s10924-020-01697-9

Chen, Z. H., Liu, W. C., Boukhair, M., Bakri, M. K.B., Li, H., and Zhang, S. B. (2025). "Engineering strong and tough wood fiber/polyhydroxybutyrate bio-composite: Synergistic modification, performance optimization, and mechanistic insights," *Composites Part B: Engineering* 295, article 112174. DOI: 10.1016/j.compositesb.2025.112174

Elsheikh, A. H., Panchal, H., Shanmugan, S., Muthuramalingam, T., El-Kassas, A. M., and Ramesh, B. (2022). "Recent progresses in wood-plastic composites: Pre-processing treatments, manufacturing techniques, recyclability and eco-friendly assessment," *Cleaner Engineering and Technology* 8, article 100450. DOI: 10.1016/j.clet.2022.100450

GB/T 1040.1 (2006). "Plastics – Determination of tensile properties – Part 1: General principles," Standardization Administration of China, Beijing, China.

GB/T 1043.1 (2008). "Plastics – Determination of Charpy impact properties – Part 1: Non-instrumented impact test," Standardization Administration of China, Beijing, China.

GB/T 17657 (2022). "Test methods of evaluating the properties of wood-based panels and surface decorated wood-based panels," Standardization Administration of China, Beijing, China.

Guo, L. F., Meng, A. J., Wang, L. Z., Huang, J., Wang, X. J., Ren, H., Zhai, H. M., and Ek, M. (2020). "Improving the compatibility, surface strength, and dimensional stability of cellulosic fibers using glycidyl methacrylate grafting," *Journal of Materials Science* 55(27), 12906-12920. DOI: 10.1007/s10853-020-04932-9

Gupta, B. S., Reiniati, I., and Laborie, M-P. G. (2007). "Surface properties and adhesion of wood fiber reinforced thermoplastic composites," *Colloids and Surfaces A: Physicochemical and Engineering Aspects* 302(1-3), 388-395. DOI: 10.1016/j.colsurfa.2007.03.002

Han, X. X., Huang, L. J., Wei, Z. H., Wang, Y. A., Chen, H. B., Huang, C. X., and Su, S. Z. (2021). "Technology and mechanism of enhanced compatibilization of polylactic acid-grafted glycidyl methacrylate," *Industrial Crops and Products* 172, article 114065. DOI: 10.1016/j.indcrop.2021.114065

Huang, B., Chen, L., Wang, X. K., Ma, X. X., Liu, H. R., Zhang, X. B., Sun, F. B., Fei, B. H., and Fang, C. H. (2023). "Eco-friendly, high-utilization, and easy-manufacturing bamboo units for engineered bamboo products: Processing and mechanical characterization," *Composites Part B: Engineering* 267, article 111073. DOI: 10.1016/j.compositesb.2023.111073

Hubbe, M. A., Lavoine, N., Lucia, L. A., and Dou, C. (2021). "Formulating bioplastic composites for biodegradability, recycling, and performance: A review," *BioResources* 16(1), 2021-2083. DOI: 10.15376/biores.16.1.Hubbe

Jiang, W. R, Bao, R. Y., Liu, Z. Y., Yang, W., Xie, B. H., and Yang, M. B. (2013). "Structure and properties of PLA-*g*-MAH compatibilized modified PLA/PETG blends," *Polymer Materials Science and Engineering* 29(03), 107-110. DOI: 10.16865/j.cnki.1000-7555.2013.03.026

Khamedi, R., Hajikhani, M., and Ahmaditabar, K. (2019). "Investigation of maleic anhydride effect on wood plastic composites behavior," *Journal of Composite Materials* 53(14), 1955-1962. DOI: 10.1177/0021998318816769

Lainé, C., Bounor-Legaré, V., Monnet, C., and Cassagnau, P. (2008). "Free radical polymerization of glycidyl methacrylate in plasticized Poly(vinyl chloride)," *European Polymer Journal* 44(10), 3177-3190. DOI: 10.1016/j.eurpolymj.2008.07.004

Liu, C. H., Yuan, W. Y., Ma, W. L., Yang, M., Yang, M., Cui, L. M., and Guan, C. J. (2024). "Influence of carboxy-terminated hyperbranched polyester and polyethylene glycol on the mechanical and thermal properties of polylactic acid/straw flour composites," *International Journal of Biological Macromolecules* 279(1), article

135226. DOI: 10.1016/j.ijbiomac.2024.135226

Liu, L., Bai, S. Q., Yang, H. Q., Li, S. B., Quan, J., Zhu, L. M., and Nie, H. L. (2016). "Controlled release from thermo-sensitive PNVCL-co-MAA electrospun nanofibers: The effects of hydrophilicity/hydrophobicity of a drug," *Materials Science & Engineering C-Materials for Biological Applications* 67, 581-589. DOI: 10.1016/j.msec.2016.05.083

Luo, S. H., Xiao, Y., Lin, J. Y., Chen, Z. H., Lin, S. T., and Wang, Z. Y. (2022). "Preparation, characterization and application of maleic anhydride-modified polylactic acid macromonomer based on direct melt polymerization," *Materials Today Chemistry* 25, article 100986. DOI: 10.1016/j.mtchem.2022.100986

Ma, Z. H., Wu, Y., Wang, H. Y., Zhang, J., and Yuan, S. F. (2025). "The effect of plasma treatment on the mechanical properties of HDPE/bamboo fiber composites," *Polymers* 17(7), article 983. DOI: 10.3390/polym17070983

Martel, B., Thuaut, P. L., Crini, G., Morcellet, M., and Torri, G. (2000). "Grafting of cyclodextrins onto polypropylene nonwoven fabrics for the manufacture of reactive filters. II. Characterization," *Journal of Applied Polymer Science* 78(12), 2166-2173. DOI: 10.1002/1097-4628(20001213)78:123.0.CO;2-4

Meng, X., Hu, F., Liu, B. Y., Cao, Y., Xu, H. L., Li, L. F., and Yu, L. P. (2024). "Study on the characterization of physical, mechanical, and mildew resistance properties of enzymatically treated bamboo fiber-reinforced polypropylene composites," *Forests* 15(1), article 60. DOI: 10.3390/f15010060

Omodunbi, A. A. (2021). "The recent development in the syntheses, properties, and applications of triple modification of various starches," *Starch-Stärke* 73(3-4), article 2000125. DOI: 10.1002/star.202000125

Parikh, H. H., Chokshi, S., Chaudhary, V., Oza, A. D., and Prakash, C. (2024). "Development and characterization of eco-friendly extruded green composites using PLA/wood dust fillers," *Proceedings of the Institution of Mechanical Engineers, Part J: Journal of Engineering Tribology* 238(6), 676-686. DOI: 10.1177/13506501241233628

Pérez, J. M., Ruiz, C., and Fernández, I. (2022). "Synthesis of a biodegradable PLA: NMR signal deconvolution and end-group analysis," *Journal of Chemical Education* 99(2), 1000-1007. DOI: 10.1021/acs.jchemed.1c00824

Prasad, J. J. V., and Kumar, S. P. (2016). "A review of recent developments in natural fibre composites and their mechanical performance," *Composites Part A: Applied Science and Manufacturing* 83, 98-112. DOI: 10.1016/j.compositesa.2015.08.038

Rajeshkumar, G., Seshadri, S. A., Devnani, G. L., Sanjay, M. R., Siengchin, S., Maran, J. P., Al-Dhabi, N. A., Karuppiah, P., Mariadhas, V. A., Sivarajasekar, N., and Anuf, A. R. (2021). "Environment friendly, renewable and sustainable poly lactic acid (PLA) based natural fiber reinforced composites-A comprehensive review," *Journal of Cleaner Production* 310, article127483. DOI: 10.1016/j.jclepro.2021.127483

Rajgond, V., Mohite, A., More, N., and More, A. (2024). "Biodegradable polyester-polybutylene succinate (PBS): A review," *Polymer Bulletin* 81(7), 5703-5752. DOI: 10.1007/s00289-023-04998-w

Read, T., Chaléat, C., Laycock, B., Pratt, S., Lant, P., and Chan, C. M. (2024). "Lifetimes and mechanisms of biodegradation of polyhydroxyalkanoate (PHA) in estuarine and marine field environments," *Marine Pollution Bulletin* 209, article 117114. DOI: 10.1016/j.marpolbul.2024.117114

Rodic, P., Iskra, J., and Milosev, I. (2014). "Study of a sol-gel process in the preparation

of hybrid coatings for corrosion protection using FTIR and ^{1}H NMR methods," *Journal of Non-Crystalline Solids* 396, 25-35. DOI: 10.1016/j.jnoncrysol.2014.04.013

Sajna, V. P., Mohanty, S., and Nayak, S. K. (2016). "Effect of poly (lactic acid)-graft-glycidylmethacrylate as a compatibilizer on properties of poly (lactic acid)/banana fiber biocomposites," *Polymers for Advanced Technologies* 27, 515-524. DOI: 10.1002/pat.3698

Shu, Y., He, J., Xu, D. P., Hu, J. P., Luo, Q. L., Ouyang, Y. J., and Wan, C. X. (2025). "Mechanical and thermal behavior of PBAT matrix composites filled with lignin," *Journal of Polymer Research* 32(2), article 56. DOI: 10.1007/s10965-025-04285-4

Song, X., Wang, M., Weng, Y., and Huang, Z. G. (2017). "Effect of bamboo flour grafted lactide on the interfacial compatibility of polylactic acid/bamboo flour composites," *Polymers* 9(8), 323-323. DOI: 10.3390/polym9080323

Trivedi, A. K., Gupta, M. K., and Singh, H. (2023). "PLA based biocomposites for sustainable products: A review," *Advanced Industrial and Engineering Polymer Research* 6(4), 382-395. DOI: 10.1016/j.aiepr.2023.02.002

Wan, H., Sun, C., Xu, C., Wang, B. W., Chen, Y., Yang, Y. Q., Tan, H. Y., and Zhang, Y. H. (2023). "Synergistic reinforcement of polylactic acid/wood fiber composites by cellulase and reactive extrusion," *Journal of Cleaner Production* 434, article 140207. DOI: 10.1016/j.jclepro.2023.140207

Wu, C. S. (2018). "Enhanced interfacial adhesion and characterisation of recycled natural fibre-filled biodegradable green composites," *Journal of Polymers and the Environment* 26(7), 2676-2685. DOI: 10.1007/s10924-017-1160-9

Xu, T., Tang, Z., and Zhu, J. (2012). "Synthesis of polylactide-graft-glycidyl methacrylate graft copolymer and its application as a coupling agent in polylactide/bamboo flour biocomposites," *Journal of Applied Polymer Science* 125(SI), E622-E627. DOI: 10.1002/app.36808

Zhang, L., Lv, S. S., Sun, C., Wan, L., Tan, H. Y., and Zhang, Y. H. (2017). "Effect of MAH-*g*-PLA on the properties of wood fiber/polylactic acid composites," *Polymers* 9(11), article 591. DOI: 10.3390/polym9110591

Zhao, Z. H., Zhang, Z. H., Wang, H. X., Li, C. F., Le, L., and Liu, M. L. (2024). "Functional wood-plastic composites: A review of research progress on flame retardancy, weather resistance and antimicrobial properties," *Industrial Crops and Products* 223, article 120196. DOI: 10.1016/j.indcrop.2024.120196

Zhou, Y., Fan, M., and Chen, L. (2016). "Interface and bonding mechanisms of plant fibre composites: An overview," *Composites Part B: Engineering* 101, 31-45. DOI: 10.1016/j.compositesb.2016.06.055

Article submitted: March 13, 2025; Peer review completed: May 2, 2025; Revised version received: May 11, 2025; Accepted: May 12, 2025; Published: May 19, 2025.
DOI: 10.15376/biores.20.3.5514-5532